# Forces on a Wall-Bound Leukocyte in a Small Vessel Due to Red Cells in the Blood Stream

Amir H. G. Isfahani and Jonathan B. Freund*
Department of Mechanical Science and Engineering, University of Illinois at Urbana-Champaign, Urbana, Illinois

ABSTRACT As part of the inflammation response, white blood cells (leukocytes) are well known to bind nearly statically to the vessel walls, where they must resist the force exerted by the flowing blood. This force is particularly difficult to estimate due to the particulate character of blood, especially in small vessels where the red blood cells must substantially deform to pass an adhered leukocyte. An efficient simulation tool with realistically flexible red blood cells is used to estimate these forces. At these length scales, it is found that the red cells significantly augment the streamwise forces that must be resisted by the binding. However, interactions with the red cells are also found to cause an average wall-directed force, which can be anticipated to enhance binding. These forces increase significantly as hematocrit values approach 25% and decrease significantly as the leukocyte is made flatter on the wall. For a tube hematocrit of 25% and a spherical protrusion with a diameter three-quarters that of the vessel, the average forces are increased by ~40% and the local forces are more than double those estimated with an effective-viscosity-homogenized blood. Both the enhanced streamwise and wall-ward forces and their unsteady character are potentially important in regard to binding mechanisms.

## INTRODUCTION

Blood behavior in vessels of diameter comparable to the blood cell size is well known to depend upon its cellular character. We assess this quantitatively for the important interactions of realistically flexible red blood cells with a wall-adhered model leukocyte at physiologically relevant flow conditions. This is a particularly important configuration in inflammation, which is well known to entail the recruitment of leukocytes to the vascular endothelium. There leukocytes must resist the forces exerted by the blood, which are expected to depend strongly upon interactions with individual blood cells, especially in small vessels. Resisting these hydrodynamic forces is necessary to establish firm adhesion and eventually transmigration.

Effects of the particulate character of blood have been studied in detail for flow in small vessels (1,2), leukocyte margination (3), leukocyte-endothelium interactions (4,5), leukocyte-leukocyte interactions (6–11), rolling of leukocytes (6,12), dynamics of vascular networks (13), and the design of blood microfluidic instruments (14–16). However, few of these studies have included three-dimensional and realistically flexible red blood cells, which is essential because of the deformations they will experience as they interact with a leukocyte in a small vessel. This deformability imbues them with a collective fluidity that affects their interactions; rigid particles are fundamentally different in this respect. Because of the predominance of red blood cells, we focus on their effects, although we anticipate that leukocyte-leukocyte interactions, though rare, might be important in the smallest vessels because of their relative size and stiffness (17).

The overall inflammation cascade starts with a trigger mechanism that instigates cellular responses with microvascular consequences. The target outcome of the cascade is to heal tissue and resolve the inflammation; however, in some cases it can also fail to resolve leading to serious chronic inflammation (18). Leukocyte margination (3,5,19,20), aggregation (21,22), rolling (17,23), attachment (23), and migration into the tissue all follow from the initial trigger. Many parts of the cascade have been studied (18), but a quantitative picture of this cascade as a whole is far from complete. Neither the average nor local unsteady forces of interaction with red cells have been quantified. We consider these here because they set the necessary strength of bonds and potentially affect the biochemical response of the leukocytes.

Suspended leukocytes are approximately spherical and relatively stiff. Both in vitro (24,25) and in vivo (10) it has been observed that they are preferentially transported toward the vessel wall (5,19,20), presumably via hydrodynamic interactions with the relatively smaller and more flexible red blood cells (3). In the absence of red blood cells, leukocytes are not observed to attach to the endothelium in postcapillary venules (26). After margination leads to contact, neutrophils in particular attach to and accumulate in postcapillary venules, which are typically 10–12 $\mu$m in diameter. The force and torque exerted on the neutrophil deform it into a teardrop-like shape (27) and cause it to roll along the vessel wall. The rolling velocity is a function of shear rate (28,29) and the distribution and tethering of selectins (30). In general, the number of adhered leukocytes decreases with increasing shear rates (24,28).

*Submitted June 17, 2012, and accepted for publication August 29, 2012.*

*Correspondence: jbfreund@illinois.edu

Editor: James Grotberg.



0006-3495/12/10/1604/12 $2.00

http://dx.doi.org/10.1016/j.bpj.2012.08.049

Our study is designed to analyze the stage just after the leukocyte has first adhered to the vessel wall. It is assumed to be either firmly adhered and stationary or rolling so slowly that its motion is negligible compared to that of the freely flowing blood. From this stage, firm adhesion to the endothelium is achieved by activation of integrins on the leukocyte and receptors such as ICAM-1 and VCAM-1 on the endothelium (31,32). Interfering with this stage could interrupt inflammation and therefore be used as a therapeutic intervention (33). It is thus important to understand the types and magnitudes of the forces acting on an adhered leukocyte. The adhesion forces generated by the receptor-ligand bonds must resist the hydrodynamic forces from the flow (34,35), including interactions with any suspended flowing blood cells (7).

In the final inflammation stage, leukocytes spread out and can project a pseudopod, which eventually leads to extravasation through the endothelium. We will also consider nonspherical configurations of the leukocyte studied as a model for assessing the forces the cell experiences as it flattens. As the leukocyte profile normal to the flow decreases, the hydrodynamic forces it experiences are likewise anticipated to decrease. We can further anticipate that this decrease will be particularly significant in small vessels where the gap size depends strongly on the leukocyte geometry. In this case, a small flattening of the leukocyte should allow red blood cells to pass it with significantly less resistance.

The forces on the leukocyte are particularly important in that they set the necessary strength of adhesion for capture and arrest. However, leukocytes are also well known to respond biochemically to force stimuli, and we also quantify forces in this regard. After firm adhesion, transmigrating neutrophils (and monocytes) with cyclic projection of pseudopods actively retract these pseudopods in response to shear (36). However, when deactivated, neutrophils can project pseudopods in response to shear (37). This behavior seems to depend on the presence of red blood cells (38), and interactions with the flowing cells are potential candidates causing this behavior. Similarly, neutrophils adhered through $\beta_2$ integrins readily respond to fluid shear but those attached via $\beta_1$ integrins respond less (39). The actual forces due to this shear—what the cell actually senses—will depend upon its interactions with the cells passing it in the sheared flow.

It is also understood that it is not just the most obvious, and probably strongest, streamwise directed hydrodynamic force that is important. Studies have indicated that normal forces on a wall-bound leukocyte, especially in the smallest of the capillaries, are potentially important (40,41). The adhesion dynamics model of Chang and Hammer (42) anticipates that all components of the force on the adhered leukocyte are important, because they all can couple with binding kinetics. This provides motivation for our investigation, particularly calculation of the wall-normal component of the forces experienced by the leukocyte. We quantify specifically how the cellular character of blood leads to forces both toward and away from the vessel wall.

A complete understanding depends upon the specific stresses experienced by the cell, which cannot be estimated, as we show, with homogeneous models of blood. Different mechanisms for mechanosensing of shear have not explained the high level of specificity in the response of different cells, perhaps because of a too simple description of the detailed forces they experience in a sheared cellular blood flow. Several studies have considered flows of homogeneous, Newtonian, or non-Newtonian fluids, over adhered leukocyte. Forces have been inferred in vivo based on differential pressures across the leukocyte and Newtonian shear stress (34,41,43). However, the well-understood properties of the Newtonian-fluid flow equations in the low-Reynolds-number limit guarantee that the flow about a sphere will be fore-aft symmetric, with exactly antisymmetric pressure and zero net force directed toward the vessel wall. Numerical investigations of homogeneous non-Newtonian flow over adhered leukocytes (44,45) can break this symmetry but cannot represent the details of the particulate character of blood expected to be important at this scale. To estimate the effect of this, rigid-sphere models of red blood cells (46), rigid two-dimensional (2D) ellipsoids (47,48), and rigid 2D rectangular with hemispherical caps (47) have been simulated. Experimentally, red blood cells have been modeled as gelatin pellets (49) and elastic (50) and rubber (51,52) discs. These all significantly enhance forces, but none of the materials used approach the fluidity of a realistically flexible red blood cell, as we employ here with our validated simulation model (53,54).

Wang and Dimitrakopoulos (41) investigated different components of the forces acting on a protuberance attached to a tube wall in a Newtonian viscous flow. In larger vessels, the Newtonian homogeneous assumption is better justified than in small capillaries (45). The flowing red blood cells are not considered but are thought to have an enhancing effect on the findings (47). They conclude that the normal component of the force is more significant for the less spread cells (41,55,56). Spreading of the cells, or lack thereof, has a greater effect in small vessels as opposed to the arteries and veins (57). Both endothelial and leukocytes may spread into different shapes (37). We shall see the same trends in the Results section; however, the magnitude of the forces is magnified by the presence of red blood cells.

In the following section, we present the geometry of the model microvessel and the wall-attached model of a leukocyte, the red blood cell model, and provide a synopsis of the numerical solver used. In the Results section, we present results for the forces on a wall-bound leukocyte and how their different components are affected by the flow of red blood cells. These are contrasted with a homogeneous Newtonian flow model.

## TECHNIQUES

### Physical model

The simulation setup is shown schematically in Fig. 1. A pressure gradient $\langle -\partial p/\partial z \rangle$ drives flow in the $+z$ -direction with prescribed tube-averaged velocity $\langle U_z \rangle_t$. The tube and leukocyte-sphere diameters are $D_t$ and $D_s$, respectively, and no glycocalyx surface layer is included in the model, though it might affect some of the detailed results in vivo (58). The streamwise periodic length of the tube is $L_z$. The angle $\theta$ parameterizes how flattened the leukocyte is on the vessel wall. For these simulations we specify the volumetric flow rate in the tube; a constant driving pressure condition documented elsewhere (59) shows similar results, unless it is so low that the cells are effectively stopped by the leukocyte. For all the cases here, volumetric flow rate is $Q = 28181\ \mu\text{m}^3/\text{s}$, which corresponds to an average (over the tube cross section) tube velocity of $\langle U_z \rangle_t = 282\ \mu\text{m/s}$. This corresponds to a pseudoshear rate of $U_z/D = 25\ \text{s}^{-1}$. This rate is in the range observed (60,61) and above the rate at which aggregation is thought to play a significant role (62). We neglect any red blood cell aggregation or molecular interactions with the leukocyte. Higher speeds and shears are observed in some vessels of this size, but the blockage caused by the leukocyte is expected to suppress flow, which led us to this value. At these scales and flow rates, Reynolds numbers are $Re \lesssim 0.01$; therefore, inertia is neglected.

Each red blood cell is modeled as an elastic shell enclosing a Newtonian fluid of viscosity $\lambda = 5$ times that of the blood plasma (63), as has been used in previous red cell models (64). The elastic shell is assumed to be governed by a finite deformation constitutive law (65) with shear modulus $E_s = 4.2 \times 10^{-6}$ N/m and bending modulus $E_b = 1.8 \times 10^{-19}$ N·m. A large dilation modulus ($E_d = 67.7 \times 10^{-6}$N/m) is used to model the strong 2D near incompressibility of the red-cell membrane. These elastic parameters match those developed by Pozrikidis (64) based upon experimental data. We neglect membrane viscosity, and show that the interior viscosity is sufficient to reproduce the gross relaxation time of a red blood cell (59). Finite membrane viscosity would be expected to further increase forces on the leukocyte beyond what we compute here. Complete details of our formulation of this model have been reported elsewhere (54).

Lubrication theory would preclude cell-cell contact, but finite numerical accuracy makes it possible, though it is rare given the high accuracy used in these simulations. These rare contacts are avoided by an ad hoc constraint (54). The minimum separation distance $\delta$ is 56 nm or $0.01\ d_o$. Zhao et al. (54) show that the pressure drop in a round tube changes by $<2\%$ by doubling and halving this distance. At such scales, molecular interactions become important, therefore resolving the lubrication films at closer separations would not necessarily improve the physical realism of the model (2).

The tube diameter is $D_t = 11.28\ \mu\text{m}$, which is at the particularly small end of what might be considered a venule (60,66), and the leukocyte-sphere has diameter $D_s = 8.46\ \mu\text{m}$, both of which are within the physiological range for capillaries and neutrophils. These correspond to a tube with $D_t = 2\ d_o$, where $d_o$ is a sphere that matches the volume of a typical red blood cell ($94\ \mu\text{m}^3$). The leukocyte model thus has diameter $D_s = 1.5\ d_o = 0.75\ D_t$. The periodic length of the tube is $L_z = 25.38\ \mu\text{m} = 3.0\ D_s$, so there is a $2D_s$ distance between the leukocyte and its periodic image. For the single-cell case, the effect of nearly doubling the periodic length of the tube to $L_z = 44.53\ \mu\text{m}$ increases the forces we report in this work by ~10% (59), which we deemed to be acceptable for the current study. Decreasing the length by 50% to $L_z = 18.21$ causes much more significant (a factor of two decrease in cases) changes (59).

Previous studies (41,55) have shown, as expected, that the leukocyte protrusion distance across the tube significantly affects the forces that it experiences. To study this for some cases, we vary the angle $\theta$ it makes with the vessel wall, as defined in Fig. 1, while keeping the volume of the

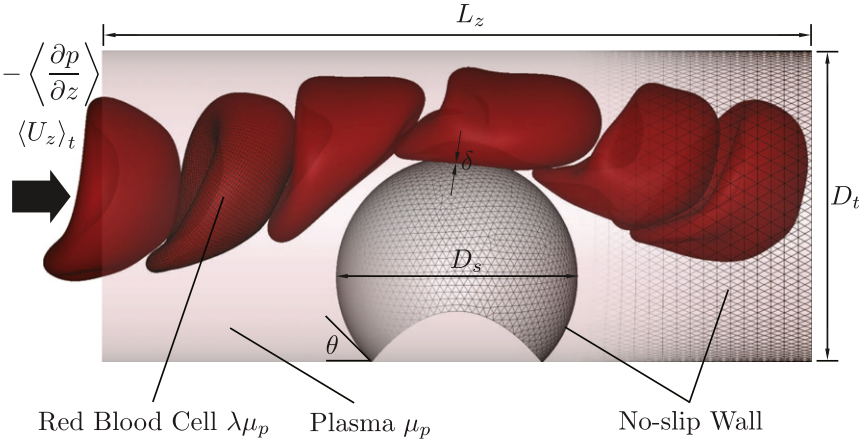


FIGURE 1 Simulation configuration.

leukocyte constant. For our baseline configurations we take a spherical $\theta = 0$ leukocyte, as visualized in Fig. 1.

### Numerical discretization

The flexibility of the red blood cells is of utmost importance for this study. The solver must be able to represent efficiently the significant deformations the cells experience as they flow through the tight confines of the model vessel. The full details of the red blood cell representation and the overall boundary integral algorithm employed to do this are reported in publications specifically on these methods (53,54), and are therefore only summarized here. Each red blood cell is represented by a set of advected collocation points that are interpolated by spherical harmonic basis functions to calculate the elastic stresses in the cells. These membrane stresses balance forces exerted by the membrane on the plasma and cell-interior fluid, which in turn affect fluid flow. The flow is calculated using boundary integrals: the motion of the collocation points depends upon the tractions exerted on the fluid by all the cells and surfaces in the domain. This $n$-body-like system, which would be expensive to compute, is approximated accurately using the particle mesh Ewald method, developed for electrostatic interactions (67,68) and extended to Stokes flow (69,70). With this approach, the Green's functions of the Stokes operator are decomposed into short-range and smooth components, the second of which can be efficiently evaluated on a regular mesh using Fourier methods. These interactions lead to an $O(n \log n)$ operation count with a total number of collocation points, $n$. The spectral basis functions make the algorithm accurate and the particle mesh Ewald implementation for the solution renders it efficient. Stability is achieved not by numerical dissipation, which degrades the fidelity of the discretization, but by a dealiasing procedure (53,54). This mitigates challenging nonlinear instability mechanisms without degrading the fidelity of the resolved modes of the simulation. Once the resolution is set by the user for a desired accuracy, stability is ensured independently by this procedure.

The geometry in Fig. 1 is represented by 6588 triangular elements on the tube with side lengths ~564 nm and 6147 elements on the leukocyte with side lengths ~282 nm. As discussed elsewhere in detail (54), a single-layer potential is used to enforce the no-slip condition. The maximum wall relative residual velocity in solving for the wall traction force is $\lesssim 10^{-4}$, which typically requires up to ~20 GMRES iterations (71). The forces on the wall-bound cell are insensitive to the wall mesh resolution, as determined through comparison with results for finer surface meshes (59).

Each red blood cell was discretized with $N = 24$ spherical harmonics, which corresponds to $N^2 = 1152$ degrees of freedom per coordinate direction. A dealiasing factor (53,54) of three was used for these simulations. The simulations presented here required up to several days on 16 processor cores. The poor parallel scalability of three-dimensional fast Fourier transforms somewhat limits the parallel scalability of the algorithm. More details about practical details of the simulations and more specific runtimes are available elsewhere (59).

## RESULTS

### Homogeneous Newtonian blood model

To provide a point of comparison for the forces exerted on the wall-bound leukocyte, we contrast results for the explicit cellular flow with a homogeneous Newtonian blood model, evaluated with the same solver but without red blood cells. In these cases, a viscosity for the assumed homogeneous fluid must be chosen. We consider several viscosities for this fluid. One is the plasma viscosity, though the cells surely elevate the resistance beyond this. We also use the bulk viscosity of blood at the same $H_T$, as would be used in a large-scale flow where blood is expected to be approximately Newtonian. Another option is the effective viscosity, as extensively documented for flow in round tubes by Pries et al. (61). The effective viscosity is the Newtonian viscosity that would be deduced from flow rate-pressure drop measurements were the fluid Newtonian. However, in small confines, such as we consider, these experiments show a strong sensitivity of this effective viscosity to tube diameter. Recent simulations also show a strong sensitivity to shear rate for tubes of the diameter considered in this work (2). Thus, this viscosity, although a reasonable numerical value to choose, is usually used to show deviations from Newtonian fluid behavior. For this reason, we do not use it, but instead, and in the same spirit, we report and compare the homogeneous models with the Newtonian viscosity that would produce the same net streamwise force on the leukocyte. However, we anticipate that the flow details will be very different even in this case. For example, no Newtonian-fluid model will predict a finite force toward or away from the vessel wall, as discussed in the Introduction section. Likewise, there will be no lateral forces for an exactly Newtonian fluid. We shall see that both of these forces have significant unsteady fluctuations for the cellular blood flow we simulate.

### Forces with cellular blood flow

We study in detail two basic configurations; subsequent sections will compare these baseline cases to cases in which $H_T$ and leukocyte flatness (contact angle $\theta$) are varied. The first of these baseline cases has a single red blood cell passing the wall-bound leukocyte, which for the specified tube length $L_z = 25.4$ $\mu$m corresponds to $H_T = 4.3$ %, and the other has six cells and thus $H_T = 25.4\%$. Hematocrit values are observed both lower (72) and higher (66), and we take this value to be representative (73,74). In the

single-cell case, the cell is initialized on the center of the tube. For the $H_T = 25\%$ case, the cells are initiated in random positions in their equilibrium biconcave discoid shape, but they deform and become independent of this artificial initial condition before any statistics are analyzed.

Components of the traction (force per unit area) on the surface of the wall-bound leukocyte are calculated using the same second-order accurate seven-point Gauss quadratures (54,75) used in the computation. These are plotted in Fig. 2 for the one red blood cell case and see Fig. 4 for the six red blood cell $H_T = 25\%$ case.

The surface-averaged mean traction in the $i$th direction is

$$\langle f_i \rangle = \frac{1}{A_s} \int_{A_s} f_i ds, \tag{1}$$

where $A_s$ is the surface of the wall-bound leukocyte. Although a typical homogeneous blood model would predict the lateral $x$ and wall-normal $y$ components to be zero, fluctuations due to the cells are clearly seen in Figs. 2 *a*, 4 *a* and *b*. For the one-cell case, because the red blood cell was initiated on the axis of symmetry, $\langle f_x \rangle$ is effectively zero for our simulations, though this would not be the case in general.

In the $H_T = 25\%$ case, the red blood cells pass the leukocyte approximately one at a time in a roughly side-to-side fashion. As it passes on one side, each cell exerts a net force toward the other side. This is most pronounced in Fig. 5 *f* and *h*, which correspond to points at the lateral force extrema in Fig. 2 *a*. The most extreme of these mean tractions is 0.4 Pa, which correspond to lateral forces of 90 N. The maximum forces are twice that expected for just plasma, though less than that for a Newtonian bulk blood viscosity for the same $H_T$.

For both cases there is a force toward the wall that would potentially stabilize adhesion by reducing strain on the binding molecules. These downward directed tractions for the single red blood cell are as high as 0.95 Pa, which corresponds to a net wall-ward force of 213.6 pN. For $H_T = 25\%$, these values are between 0.72 and 1.15 Pa (or 161.9–258.6 pN). However, in the case of a single red blood cell, these interactions also pull the leukocyte off the vessel wall. The upward force is exerted as the red blood cell is about to enter the region above the leukocyte, as can be seen in Fig. 3 *c* and the corresponding ◦ point in Fig. 2 *a*. The downward forces, which are thought to cause the leukocyte to penetrate the glycocalyx (58), significantly favor adhesion (4,5,10), enabling more bonds that cannot be broken by the consequent pull. In adhesion modeling (42,58,76,77), if the height of a ligand drops below a critical value, bond formation is triggered. These downward forces can be seen at their maximum in Fig. 3 *f* and its corresponding ◦ point in Fig. 2 *a* for the single-cell case and in Fig. 5 *b*, *d*, *f*, *h*, and *j* for the corresponding ◦ points in Fig. 4 *b*, for $H_T = 25\%$. In all of the instances, when the surface-averaged wall-ward force is at its peak, a red blood cell is directly above the leukocyte. For the single-cell case, local maximum tractions are up to 3.71 and 2.03 times larger than the apparent-viscosity-homogenized model during the negative and positive lift exertions, respectively. In contrast,

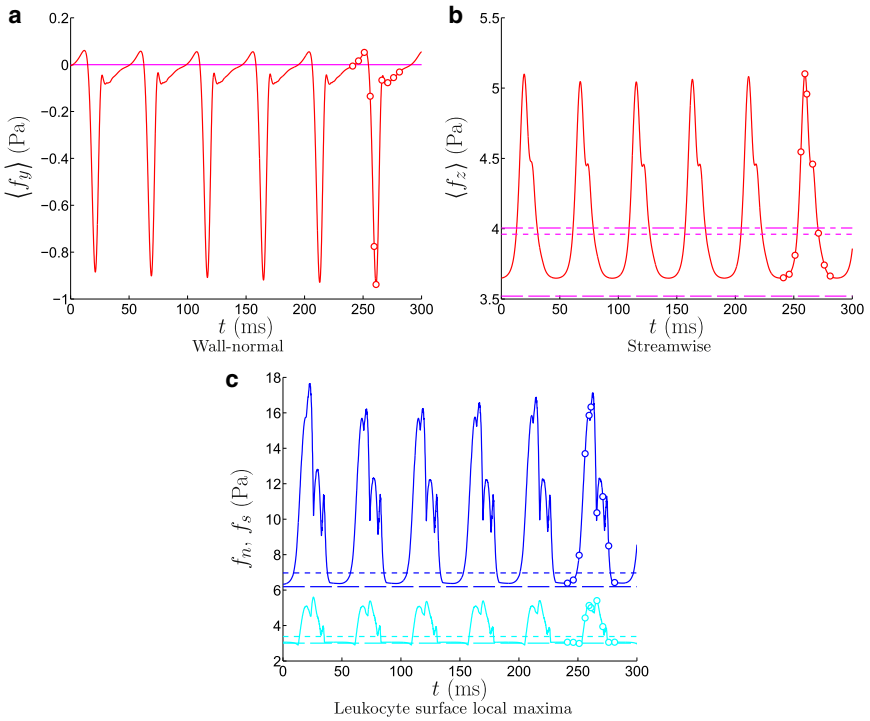


FIGURE 2 Time histories of surface averaged tractions (1) in the (*a*) wall-normal $\langle f_y \rangle$ and (*b*) streamwise $\langle f_z \rangle$ direction; and (*c*) the maximum leukocyte-normal $f_n$ and shear $f_s$ tractions. The straight lines show homogeneous blood models with – – – the plasma viscosity, - - - - the bulk blood viscosity, and – - – the viscosity matching mean streamwise force. The ◦ mark times visualized in Fig. 3.

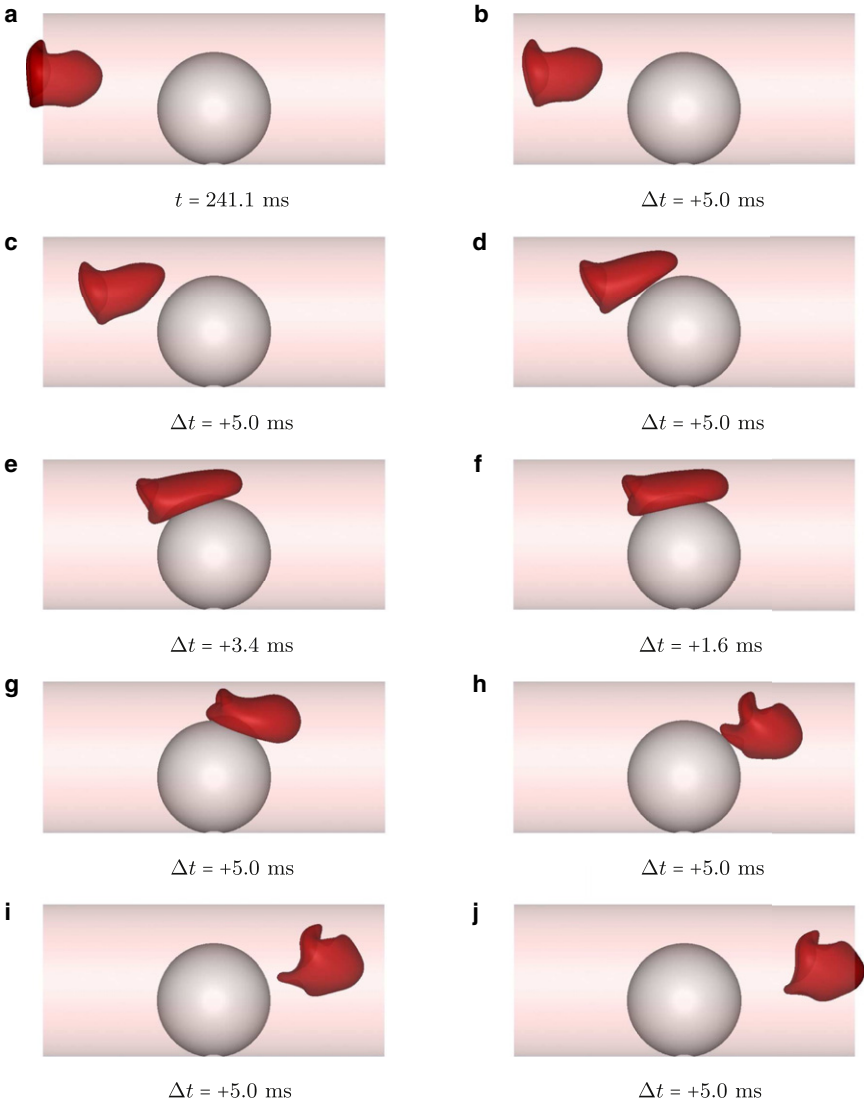


FIGURE 3 Visualization of the cell at times marked by the circle in Fig. 2. See also Movie S1 in the Supporting Material.

for $H_T = 25\%$, the maximum tractions are all in the form of a wall-directed force (a negative lift) on the leukocyte. The enhancement in these maximum tractions is on average 2.88 and at most 5.48 times those from the corresponding apparent-viscosity-homogenized model. This suggests that a single red cell might be more effective at lifting a leukocyte off the wall than a train of cells, which should be considered in adhesion modeling. It has been demonstrated that hydrodynamic interactions with suspended spherical models of cells can indeed affect the binding dynamics and cell rolling behavior (7).

The axial tractions in Figs. 2 *b* and 4 *c* show significant increases both for averaged and maximum pointwise stresses. The maximum average streamwise traction in the flow-by denoted by ◦ points on Fig. 2 *b* occurs as the red blood cell passes the gap, Fig. 3 *e*. This blockage leads to an increase in the pressure gradient to maintain the constant flow rate. The streamwise hydrodynamic force on the leukocyte is 79.1 pN for plasma, and 154.2 pN, from a homogeneous blood with a bulk viscosity of 1.95 (61,78) for $H_T = 25\%$ at this tube diameter. The shapes of the time histories of the axial traction for a single red cell are qualitatively similar to the time histories for a 2D flow of rigid ellipses past a circular leukocyte model (47) in that two consecutive peaks were observed per red blood cell pass. One peak corresponds to the cell entering the gap and the other is the red blood cell leaving the surface of the leukocyte. There is an increase in the average tractions in the axial direction of up to 45% and 86% for the single red blood cell and $H_T = 25\%$ cases relative to plasma. The single-cell case shows an increase in the average tractions in the axial direction of up to 29% relative to a homogeneous blood with a bulk viscosity of $1.35 \times 10^{-3}$ Pa·s (61,78). The homogeneous viscosities that would generate the same mean axial traction would be $1.36 \times 10^{-3}$ Pa·s and $1.62 \times 10^{-3}$ Pa·s. In terms of the maximum tractions, the increases

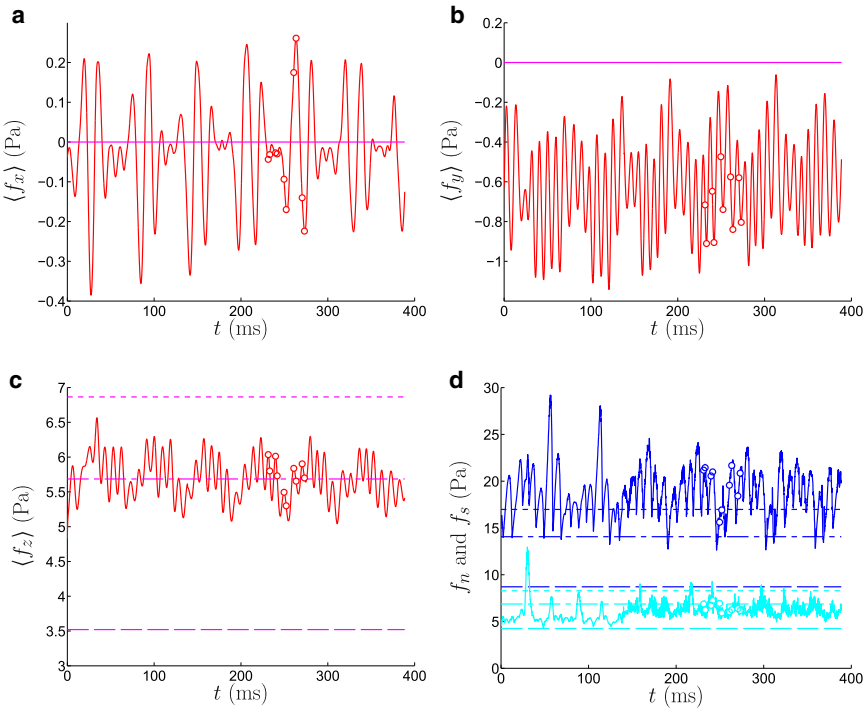


FIGURE 4 The six-cell $H_T = 25.38\%$ with curves as labeled in Fig. 2. The ◦ mark points visualized in Fig. 5.

relative to homogeneous models are up to 101% and 230% relative to plasma and 78% and 70% relative to a blood model that has been homogenized by its bulk viscosity.

Direct comparison to experiment is hindered by the challenge of measuring such small forces as these scales. However, Chapman and Cokelet (51) present experimental results for a case with red blood cells modeled by rubber discs, which can be compared with a configuration presented in the next section. In this case $D_s = 8.46$ and $D_t = 16.82$ and therefore, $D_s/D_t = 0.5$. Based on their experiments for this $D_s/D_t$ ratio and 40% hematocrit, they obtain a drag force equal to 178.1 pN for an average tube velocity of $\langle U_z \rangle_t = 125.21$ $\mu$m/s. For the same geometry but with $H_T = 25\%$, our time-averaged surface-averaged axial traction, $\langle \sigma_z \rangle$, is 0.54 Pa from simulations. This yields a drag of 121.2 pN, which is 32% lower than the experimental value. However, the experiments were performed at $H_T = 40\%$, which corresponds to an apparent viscosity that is 20% higher than the one at $H_T = 25\%$ (61). We have also observed in our studies that stiffer model cells (in the case of the experiment) exert larger forces on the wall-bound cell (59).

Figs. 2 *c* and 4 *d* show the maximum normal and shear stresses that the leukocyte experiences. The normal stresses in the single-cell case are up to 2.8 times that of plasma and 2.5 times the normal stresses from the bulk-viscosity-homogenized model. The corresponding amplifications for shear stress are factors of 1.9 and 1.7, respectively. When $H_T = 25\%$, the maximum normal stresses are 3.4 times what plasma would exert and 1.7 times that of the bulk-viscosity-homogenized model. Shear stresses at one point during the simulation are 3.0 and 1.6 times plasma and bulk-viscosity-homogenized, however the next peaks are 2.2 and 1.1 times plasma and bulk-viscosity-homogenized.

In all cases, the increase in the tractions on the wall-bound leukocyte is due to the particulate character of blood. Clearly a homogeneous model, even if the viscosity is elevated to that of blood rather than plasma, will neglect key features of the forces on the leukocytes. In the Dependence on hematocrit section, we examine dependence upon $H_T$ and in the Dependence on leukocyte geometry section we vary the leukocyte geometry.

## Dependence on hematocrit

Starting with the single-cell case, we increase the number of red blood cells in increments up to $H_T = 25\%$, which corresponds to the second case. For lower $H_T$, we do not expect significant change from the prediction based on a Newtonian plasma model, except when the cell is passing the leukocytes, which happens more frequently at higher $H_T$. This is clear for the one-cell case in Fig. 2. We therefore focus on the peak forces on the leukocyte as the cells pass, for both the local traction and the surface averaged traction as defined in (1). Despite the streamwise periodicity of the model microvessel, none of the flows are exactly time-periodic; therefore, we further distinguish between the average of the peaks in the time histories and the maximum peaks through the course of the entire simulations. This confirms that, at least for the periods simulated, there is no interaction that is significantly stronger than the typical interaction with

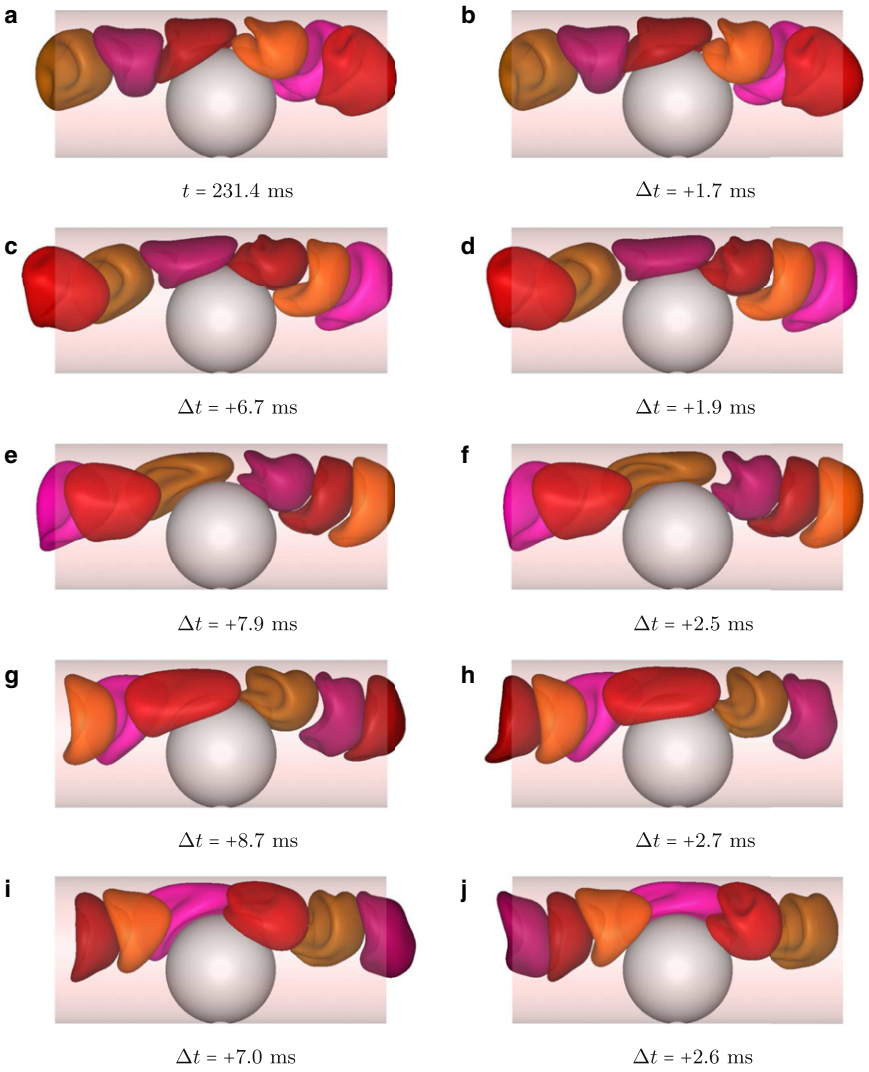


FIGURE 5 Visualization of the cells at times marked by the circle in Fig. 4. Different shadings are used to distinguish the cells. See also Movie S2.

a passing cell. These results are shown in Fig. 6. The surface averaged cell-passing peak tractions across this range of hematocrits and for this geometry are 49–115% larger than for plasma. The maximum tractions are 96–266% larger than for a Newtonian plasma-viscosity model. The effect of the cells is even more pronounced when the absolute maxima are considered throughout the duration of the simulation, shown in these same figures. Even when these forces are compared with a homogeneous model of blood with its bulk viscosity at these hematocrits, the average

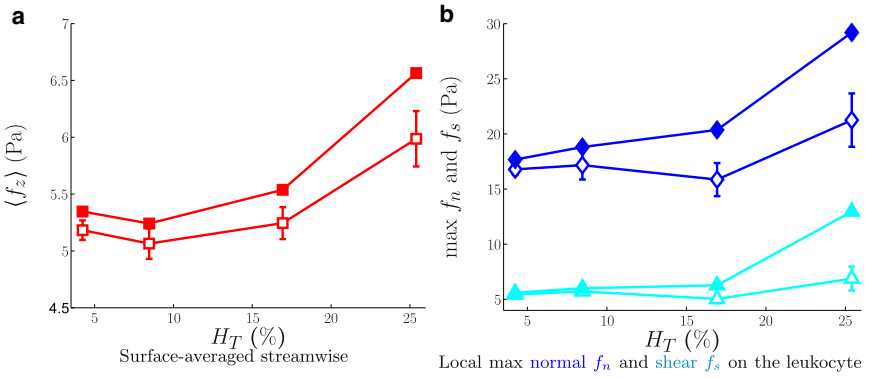


FIGURE 6 Peak surface stresses with increasing $H_T$. In all cases, we show both the average of all the peak interactions (□, ◇, and △) and absolute peaks for the simulated period (■, ◆, and ▲). The error bars show standard deviations.

tractions are still 8–32% and the maximum tractions, 49–88% larger. Therefore, for the range of hematocrits shown and at the scales of this setup, a homogeneous assumption significantly underpredicts the forces exerted on the wall-bound leukocyte.

With increasing $H_T$, the increase in surface tractions is relatively slow up to $H_T = 25\%$, with the peaks not much larger than for the single-cell case. In these cases, $H_T$ seems low enough that the cells are still able to pass in single file over the leukocyte sphere. However, we see a pronounced increase for $H_T = 25\%$, especially for the leukocyte surface shear stress. For six red cells, multiple cells interact with the leukocyte at any given time and therefore, the magnitude of the tractions starts to increase above this single-cell interaction. This can be seen in Fig. 5. In every frame at least two, and in some cases three, red blood cells are in near contact with the model leukocyte. Given how significantly the red blood cells distort as they squeeze past the wall bound leukocyte, we can anticipate that significantly less force will be exerted for larger diameter vessels, for which less distortion is required. This is indeed the case, and the expected results in this regard are reported elsewhere (59).

## Dependence on leukocyte geometry

Adhered cells are well known to depart from their approximately spherical shape (57,79,80), which will reduce the hydrodynamic forces they experience. We model this change in geometry by increasing the contact angle (Fig. 1) between the adhered cell and the vessel wall such that the leukocyte volume is constant. As the contact angle increases, the cells spread further on the inside of the tube wall. The streamwise extent of the cell increases significantly, and in these simulations the periodic length of the tube is kept three times the streamwise length of the model leukocyte. A similar mesh density is maintained on both the leukocyte and the tube as for the baseline cases (see Numerical discretization section). The configurations are shown in Fig. 7.

Fig. 8 shows the force time histories the peaks of which are time averaged in Fig. 9. These show decreasing forces with cell flattening, which approach the homogeneous blood model limit. As the contact angle between the cell and the cylindrical substrate increases from 0° to 135°, the relative increase in the average tractions compared to plasma drops from 47% to 9% for the single-cell cases (not shown) and from 70% to 35% for $H_T = 25\%$ (Fig. 9). The maximum tractions follow the same trend and drop from 102% to 12% for the single-cell cases (not shown) and from 189% to 53% for the $H_T = 25\%$ compared to plasma (Fig. 9). In the case of $H_T = 25\%$, the relative increase compared to a homogeneous model with its bulk viscosity at this hematocrit (61,78) decreases from 48% to 11% as the contact angle changes from 0° to 90°.

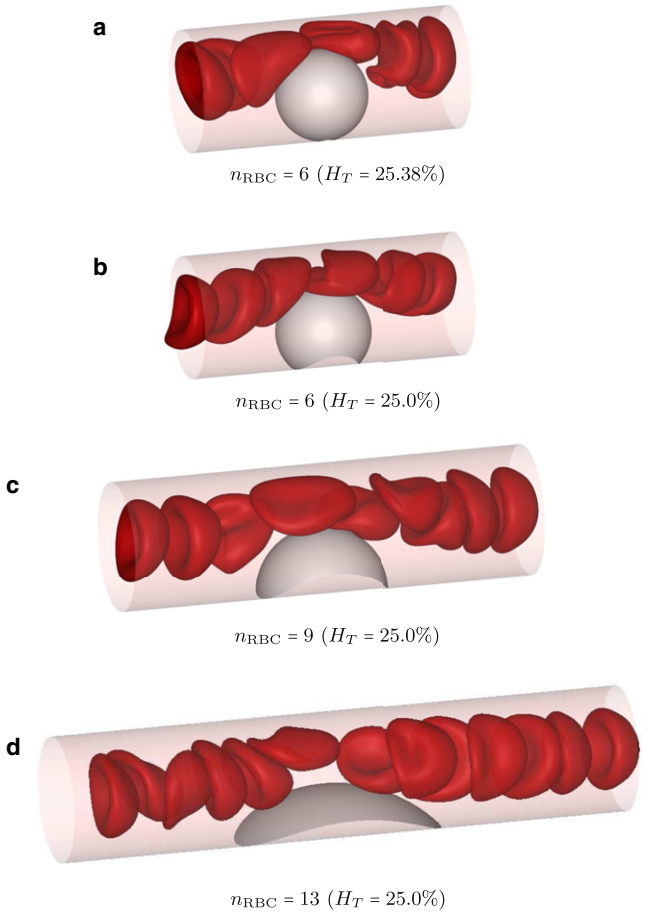


FIGURE 7 Visualizations of cases with a different leukocyte contact angle with $H_T = 25\%$.

## CONCLUSION

We have examined how red blood cells increase the mean and instantaneous forces experienced by a model wall-adhered leukocyte. The forces are well above what would be predicted with a homogeneous blood model. Depending upon the geometry and $H_T$, cellular blood can exert many times the forces predicted by corresponding homogeneous models. The cellular blood forces are also qualitatively different in that there is a net force directed toward or away from the vessel wall, which can be anticipated to interact with adhesion kinetics. For a single cell, a model for a low $H_T$ flow, this force is directed both toward the wall, which would be expected to promote adhesion, and away from it, which would inhibit it. However, for $H_T = 25\%$ the force is uniformly directed toward the wall. Furthermore, in the presence of red blood cells, the leukocyte experiences an oscillating net lateral force as the red cells pass it. As expected, the strongest overall forces are in the direction of the flow. In terms of the maximum surface tractions, which might activate or otherwise affect the leukocyte behavior for $H_T = 25\%$, the relative force increases are up to 317% for just plasma and 114% relative

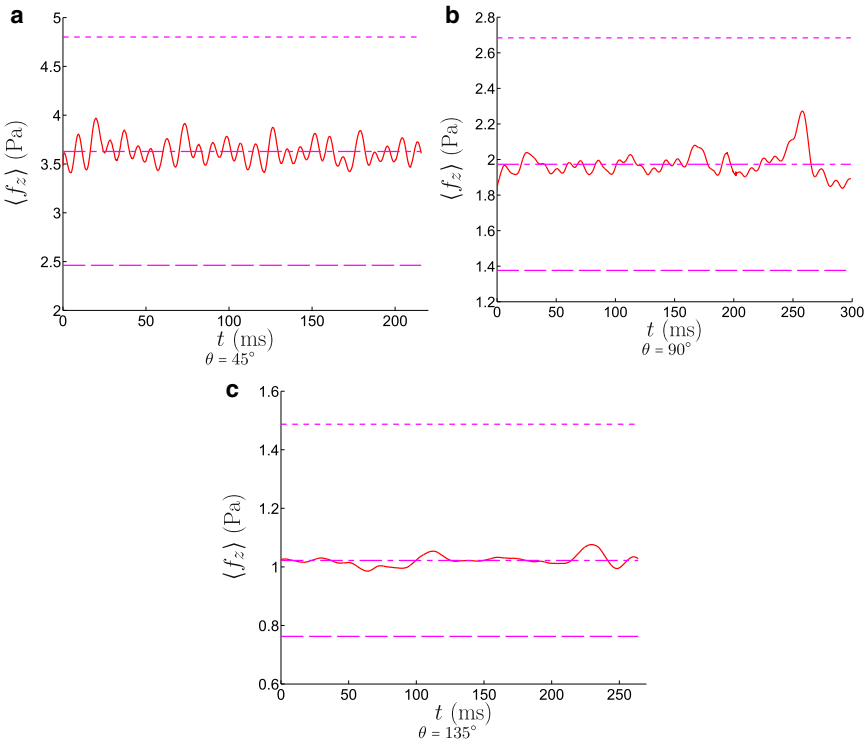


FIGURE 8 Mean streamwise forces for contact angles as labeled: (*a*) $\theta = 45°$, (*b*) $\theta = 90°$, and (*c*) $\theta = 135°$. The $\theta = 0°$ is identical to Fig. 4 *c*. The straight lines show homogeneous blood models with – – – the plasma viscosity, - - - - the bulk blood viscosity, and – - – the viscosity matching mean streamwise force.

to a blood model that has been homogenized by its bulk viscosity. The homogeneous assumption of blood, even if its viscosity is increased to reported bulk values for blood, will lead to significant errors for the configurations as presented here. These types of forces potentially lead to different signaling pathways that result in different responses from the cell (see Introduction section). The unsteady character of the forces due to the interactions with the red blood cells as they pass the bound leukocyte might also be important for binding kinetics in adhesion dynamics models, as has been observed for suspending spheres flowing past wall adhered spheres (7). The specific effect of red blood cell flexibility has not been studied, but given the distortions observed for the present geometry, we can anticipate that for this case at least more rigid cells would exert significantly stronger forces.

## SUPPORTING MATERIAL

Two movies are available at http://www.biophysj.org/biophysj/supplemental/S0006-3495(12)00976-9.

Support from the National Science Foundation (CBET 09-32607) and a fellowship from Computational Science & Engineering at the University of Illinois at Urbana-Champaign is gratefully acknowledged. This research was also supported in part by the National Science Foundation through TeraGrid resources provided by Texas Advanced Computer Center.

## REFERENCES

1. Fedosov, D. A., B. Caswell, and G. E. Karniadakis. 2010. A multiscale red blood cell model with accurate mechanics, rheology, and dynamics. *Biophys. J.* 98:2215–2225.
2. Freund, J. B., and M. M. Orescanin. 2011. Cellular flow in a small blood vessel. *J. Fluid Mech.* 671:466–490.

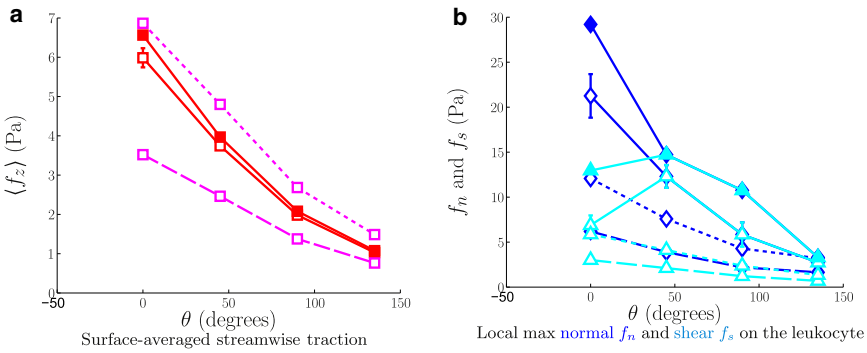


FIGURE 9 Peak surface tractions with increasing leukocyte flatness. In all cases, we show both the average of all the peak interactions, open symbols (□, ◇, and △) and absolute peaks for the simulated period (■, ◆, and ▲). Also shown are results for homogeneous blood modeled with - - - - the bulk blood viscosity and – – – plasma. The error bars show standard deviations.

3. Freund, J. B. 2007. Leukocte margination in a model microvessel. *Phys. Fluids.* 19: 023301-1–023301-12.

4. Melder, R. J., L. L. Munn, …, R. K. Jain. 1995. Selectin- and integrin-mediated T-lymphocyte rolling and arrest on TNF-alpha-activated endothelium: augmentation by erythrocytes. *Biophys. J.* 69:2131–2138.

5. Munn, L. L., R. J. Melder, and R. K. Jain. 1996. Role of erythrocytes in leukocyte-endothelial interactions: mathematical model and experimental validation. *Biophys. J.* 71:466–478.

6. King, M. R., and D. A. Hammer. 2001. Multiparticle adhesive dynamics. Interactions between stably rolling cells. *Biophys. J.* 81:799–813.

7. King, M. R., S. D. Rodgers, and D. A. Hammer. 2001. Hydrodynamic collisions suppress fluctuations in the rolling velocity of adhesive blood cells. *Langmuir.* 17:4139–4143.

8. King, M. R., M. B. Kim, …, D. A. Hammer. 2003. Hydrodynamic interactions between rolling leukocytes in vivo. *Microcirculation.* 10:401–409.

9. King, M. R., A. D. Ruscio, …, I. H. Sarelius. 2005. Interactions between stably rolling leukocytes in vivo. *Phys. Fluids.* 17: 031501-1–031501-3.

10. Melder, R. J., J. Yuan, …, R. K. Jain. 2000. Erythrocytes enhance lymphocyte rolling and arrest in vivo. *Microvasc. Res.* 59:316–322.

11. Mitchell, D. J., P. Li, …, P. Kubes. 2000. Importance of L-selectin-dependent leukocyte-leukocyte interactions in human whole blood. *Blood.* 95:2954–2959.

12. King, M. R., and D. A. Hammer. 2001. Multiparticle adhesive dynamics: hydrodynamic recruitment of rolling leukocytes. *Proc. Natl. Acad. Sci. USA.* 98:14919–14924.

13. Pries, A. R., T. W. Secomb, …, J. F. Gross. 1990. Blood flow in microvascular networks. Experiments and simulation. *Circ. Res.* 67:826–834.

14. Davis, J. A., D. W. Inglis, …, R. H. Austin. 2006. Deterministic hydrodynamics: taking blood apart. *Proc. Natl. Acad. Sci. USA.* 103:14779–14784.

15. Jain, A., and L. L. Munn. 2009. Determinants of leukocyte margination in rectangular microchannels. *PLoS ONE.* 4:e7104.

16. VanDelinder, V., and A. Groisman. 2007. Perfusion in microfluidic cross-flow: separation of white blood cells from whole blood and exchange of medium in a continuous flow. *Anal. Chem.* 79:2023–2030.

17. Kamm, R. D. 2002. Cellular fluid mechanics. *Annu. Rev. Fluid Mech.* 34:211–232.

18. Schmid-Schönbein, G. W. 2006. Analysis of inflammation. *Annu. Rev. Biomed. Eng.* 8:93–131.

19. Goldsmith, H. L., and S. Spain. 1984. Margination of leukocytes in blood flow through small tubes. *Microvasc. Res.* 27:204–222.

20. Nobis, U., A. R. Pries, and P. Gaehtgens. 1982. Rheological mechanisms contributing to WBC-margination. *In* Microcirculation Reviews I: White Blood Cells Morphology and Rheology as Related to Function. U. Bagge, G. V. R. Born, and P. Gaehtgens, editors. Nijhoff, The Hague. 57–65.

21. Nash, G. B., T. Watts, …, M. Barigou. 2008. Red cell aggregation as a factor influencing margination and adhesion of leukocytes and platelets. *Clin. Hemorheol. Microcirc.* 39:303–310.

22. Pearson, M. J., and H. H. Lipowsky. 2004. Effect of fibrinogen on leukocyte margination and adhesion in postcapillary venules. *Microcirculation.* 11:295–306.

23. Chang, K.-C., D. F. J. Tees, and D. A. Hammer. 2000. The state diagram for cell adhesion under flow: leukocyte rolling and firm adhesion. *Proc. Natl. Acad. Sci. USA.* 97:11262–11267.

24. Abbitt, K. B., and G. B. Nash. 2001. Characteristics of leucocyte adhesion directly observed in flowing whole blood in vitro. *Br. J. Haematol.* 112:55–63.

25. Abbitt, K. B., and G. B. Nash. 2003. Rheological properties of the blood influencing selectin-mediated adhesion of flowing leukocytes. *Am. J. Physiol. Heart Circ. Physiol.* 285:H229–H240.

26. Bagge, U., A. Blixt, and K. G. Strid. 1983. The initiation of post-capillary margination of leukocytes: studies in vitro on the influence of erythrocyte concentration and flow velocity. *Int. J. Microcirc. Clin. Exp.* 2:215–227.

27. Damiano, E. R., J. Westheider, …, K. Ley. 1996. Variation in the velocity, deformation, and adhesion energy density of leukocytes rolling within venules. *Circ. Res.* 79:1122–1130.

28. Firrell, J. C., and H. H. Lipowsky. 1989. Leukocyte margination and deformation in mesenteric venules of rat. *Am. J. Physiol.* 256:H1667–H1674.

29. Lipowsky, H. H., D. A. Scott, and J. S. Cartmell. 1996. Leukocyte rolling velocity and its relation to leukocyte-endothelium adhesion and cell deformability. *Am. J. Physiol.* 270:H1371–H1380.

30. Alon, R., D. A. Hammer, and T. A. Springer. 1995. Lifetime of the P-selectin-carbohydrate bond and its response to tensile force in hydrodynamic flow. *Nature.* 374:539–542.

31. Lawrence, M. B., and T. A. Springer. 1991. Leukocytes roll on a selectin at physiologic flow rates: distinction from and prerequisite for adhesion through integrins. *Cell.* 65:859–873.

32. von Andrian, U. H., J. D. Chambers, …, E. C. Butcher. 1991. Two-step model of leukocyte-endothelial cell interaction in inflammation: distinct roles for LECAM-1 and the leukocyte beta 2 integrins in vivo. *Proc. Natl. Acad. Sci. USA.* 88:7538–7542.

33. Norman, M. U., and P. Kubes. 2005. Therapeutic intervention in inflammatory diseases: a time and place for anti-adhesion therapy. *Microcirculation.* 12:91–98.

34. Gaver, 3rd, D. P., and S. M. Kute. 1998. A theoretical model study of the influence of fluid stresses on a cell adhering to a microchannel wall. *Biophys. J.* 75:721–733.

35. Hodges, S. R., and O. E. Jensen. 2002. Spreading and peeling dynamics in a model of cell adhesion. *J. Fluid Mech.* 460:381–409.

36. Moazzam, F., F. A. DeLano, …, G. W. Schmid-Schönbein. 1997. The leukocyte response to fluid stress. *Proc. Natl. Acad. Sci. USA.* 94:5338–5343.

37. Coughlin, M. F., and G. W. Schmid-Schönbein. 2004. Pseudopod projection and cell spreading of passive leukocytes in response to fluid shear stress. *Biophys. J.* 87:2035–2042.

38. Komai, Y., and G. W. Schmid-Schönbein. 2005. De-activation of neutrophils in suspension by fluid shear stress: a requirement for erythrocytes. *Ann. Biomed. Eng.* 33:1375–1386.

39. Marschel, P., and G. W. Schmid-Schönbein. 2002. Control of fluid shear response in circulating leukocytes by integrins. *Ann. Biomed. Eng.* 30:333–343.

40. King, M. R. 2006. Biomedical applications of microchannel flows. *In* Heat Transfer and Fluid Flow in Minichannels and Microchannels. S. G. Kandlikar, S. Garimella, D. Li, S. Colin, and M. R. King, editors. Elsevier, New York. 409–442.

41. Wang, Y., and P. Dimitrakopoulos. 2006. Nature of the hemodynamic forces exerted on vascular endothelial cells or leukocytes adhering to the surface of blood vessels. *Phys. Fluids.* 18: 087107-1–087107-14.

42. Chang, K. C., and D. A. Hammer. 1996. Influence of direction and type of applied force on the detachment of macromolecularly-bound particles from surfaces. *Langmuir.* 12:2271–2282.

43. House, S. D., and H. H. Lipowsky. 1988. In vivo determination of the force of leukocyte-endothelium adhesion in the mesenteric microvasculature of the cat. *Circ. Res.* 63:658–668.

44. Artoli, A. M., A. Sequeira, …, C. Saldanha. 2007. Leukocytes rolling and recruitment by endothelial cells: hemorheological experiments and numerical simulations. *J. Biomech.* 40:3493–3502.

45. Das, B., P. C. Johnson, and A. S. Popel. 2000. Computational fluid dynamic studies of leukocyte adhesion effects on non-Newtonian blood flow through microvessels. *Biorheology.* 37:239–258.

46. King, M. R., D. Bansal, …, I. H. Sarelius. 2004. The effect of hematocrit and leukocyte adherence on flow direction in the microcirculation. *Ann. Biomed. Eng.* 32:803–814.

47. Migliorini, C., Y. Qian, …, L. L. Munn. 2002. Red blood cells augment leukocyte rolling in a virtual blood vessel. *Biophys. J.* 83:1834–1841.

48. Sun, C., C. Migliorini, and L. L. Munn. 2003. Red blood cells initiate leukocyte rolling in postcapillary expansions: a lattice Boltzmann analysis. *Biophys. J.* 85:208–222.

49. Schmid-Schoenbein, G. W., Y. C. Fung, and B. W. Zweifach. 1975. Vascular endothelium-leukocyte interaction; sticking shear force in venules. *Circ. Res.* 36:173–184.

50. Schmid-Schönbein, G. W., S. Usami, …, S. Chien. 1980. The interaction of leukocytes and erythrocytes in capillary and postcapillary vessels. *Microvasc. Res.* 19:45–70.

51. Chapman, G., and G. Cokelet. 1996. Model studies of leukocyte-endothelium-blood interactions. I. The fluid flow drag force on the adherent leukocyte. *Biorheology.* 33:119–138.

52. Chapman, G. B., and G. R. Cokelet. 1997. Model studies of leukocyte-endothelium-blood interactions. II. Hemodynamic impact of leukocytes adherent to the wall of post-capillary vessels. *Biorheology.* 34:37–56.

53. Freund, J. B., and H. Zhao. 2010. A fast high-resolution boundary integral method for multiple interacting blood cells. *In* Computational Hydrodynamics of Capsules and Biological Cells. C. Pozrikidis, editor. Chapman & Hall/CRC. 71–111.

54. Zhao, H., A. H. G. Isfahani, …, J. B. Freund. 2010. A spectral boundary integral method for flowing blood cells. *J. Comput. Phys.* 229:3726–3744.

55. Sugihara-Seki, M. 2000. Flow around cells adhered to a microvessel wall. I. Fluid stresses and forces acting on the cells. *Biorheology.* 37:341–359.

56. Sugihara-Seki, M. 2001. Flow around cells adhered to a microvessel wall II: comparison to flow around adherent cells in channel flow. *Biorheology.* 38:3–13.

57. Olivier, L. A., and G. A. Truskey. 1993. A numerical analysis of forces exerted by laminar flow on spreading cells in a parallel plate flow chamber assay. *Biotechnol. Bioeng.* 42:963–973.

58. Zhao, Y., S. Chien, and S. Weinbaum. 2001. Dynamic contact forces on leukocyte microvilli and their penetration of the endothelial glycocalyx. *Biophys. J.* 80:1124–1140.

59. Isfahani, A. H. G. 2011. Forces on a wall-bound leukocyte due to flowing red blood cells. PhD thesis. University of Illinois at Urbana-Champaign, Urbana, IL.

60. Popel, A. S., and P. C. Johnson. 2005. Microcirculation and hemorheology. *Annu. Rev. Fluid Mech.* 37:43–69.

61. Pries, A. R., D. Neuhaus, and P. Gaehtgens. 1992. Blood viscosity in tube flow: dependence on diameter and hematocrit. *Am. J. Physiol.* 263:H1770–H1778.

62. Bishop, J. J., P. R. Nance, …, P. C. Johnson. 2001. Effect of erythrocyte aggregation on velocity profiles in venules. *Am. J. Physiol. Heart Circ. Physiol.* 280:H222–H236.

63. Dintenfass, L. 1968. Internal viscosity of the red cell and a blood viscosity equation. *Nature.* 219:956–958.

64. Pozrikidis, C. 2005. Axisymmetric motion of a file of red blood cells through capillaries. *Phys. Fluids.* 17: 031503-1–031503-14.

65. Skalak, R., A. Tozeren, …, S. Chien. 1973. Strain energy function of red blood cell membranes. *Biophys. J.* 13:245–264.

66. Pries, A. R., K. Ley, and P. Gaehtgens. 1986. Generalization of the Fahraeus principle for microvessel networks. *Am. J. Physiol.* 251: H1324–H1332.

67. Darden, T., D. York, and L. Pedersen. 1993. Particle mesh Ewald: an N.log(N) method for Ewald sums in large systems. *J. Chem. Phys.* 98:10089–10092.

68. Essmann, U., L. Perera, …, L. G. Pedersen. 1995. A smooth particle mesh Ewald method. *J. Chem. Phys.* 103:8577–8593.

69. Metsi, E. 2000. Large scale simulation of bidisperse emulsions and foams. PhD thesis. University of Illinois at Urbana-Champaign, Urbana, IL.

70. Saintillan, D., E. Darve, and E. S. G. Shaqfeh. 2005. A smooth particle-mesh Ewald algorithm for Stokes suspension simulations: the sedimentation of fibers. *Phys. Fluids.* 17: 033301-1–033301-21.

71. Saad, Y., and M. H. Schultz. 1986. GMRES: a generalized minimal residual algorithm for solving nonsymmetric linear systems. *SIAM J. Sci. Statist. Comput.* 7:856–869.

72. Lipowsky, H. H., S. Usami, and S. Chien. 1980. In vivo measurements of "apparent viscosity" and microvessel hematocrit in the mesentery of the cat. *Microvasc. Res.* 19:297–319.

73. Barbee, J. H., and G. R. Cokelet. 1971. The Fahraeus effect. *Microvasc. Res.* 3:6–16.

74. Goldsmith, H. L., G. R. Cokelet, and P. Gaehtgens. 1989. Robin Fåhraeus: evolution of his concepts in cardiovascular physiology. *Am. J. Physiol.* 257:H1005–H1015.

75. Pozrikidis, C. 1992. Boundary Integral and Singularity Methods for Linearized Viscous Flow. Cambridge University Press, Cambridge.

76. Dong, C., J. Cao, …, H. H. Lipowsky. 1999. Mechanics of leukocyte deformation and adhesion to endothelium in shear flow. *Ann. Biomed. Eng.* 27:298–312.

77. Hammer, D. A., and S. M. Apte. 1992. Simulation of cell rolling and adhesion on surfaces in shear flow: general results and analysis of selectin-mediated neutrophil adhesion. *Biophys. J.* 63:35–57.

78. Brooks, D. E., J. W. Goodwin, and G. V. Seaman. 1970. Interactions among erythrocytes under shear. *J. Appl. Physiol.* 28:172–177.

79. Cao, J., B. Donell, …, C. Dong. 1998. In vitro side-view imaging technique and analysis of human T-leukemic cell adhesion to ICAM-1 in shear flow. *Microvasc. Res.* 55:124–137.

80. Tözeren, A., and K. Ley. 1992. How do selectins mediate leukocyte rolling in venules? *Biophys. J.* 63:700–709.